Developmental Cell
Article

Bub1 Maintains Centromeric Cohesion by Activation of the Spindle Checkpoint

David Perera,[1] Valerie Tilston,[1] Jane A. Hopwood,[1,3] Marco Barchi,[2] Raymond P. Boot-Handford,[1] and Stephen S. Taylor[1,*]
[1]Faculty of Life Sciences, University of Manchester, Michael Smith Building, Oxford Road, Manchester M13 9PT, United Kingdom
[2]University of Rome "Tor Vergata," Department of Public Health and Cell Biology, Section of Anatomy, Room 263, Via Montpellier n.1, 00133, Rome, Italy
[3]Present address: AstraZeneca Pharmaceuticals, Mereside, Alderley Park, Cheshire SK10 4TG, United Kingdom.
*Correspondence: stephen.taylor@manchester.ac.uk
DOI 10.1016/j.devcel.2007.08.008

SUMMARY

Bub1 is a component of the spindle assembly checkpoint (SAC), a surveillance mechanism that ensures genome stability by delaying anaphase until all the chromosomes are stably attached to spindle microtubules via their kinetochores. To define Bub1's role in chromosome segregation, embryogenesis, and tissue homeostasis, we generated a mouse strain in which *BUB1* can be inactivated by administration of tamoxifen, thereby bypassing the preimplantation lethality associated with the Bub1 null phenotype. We show that Bub1 is essential for postimplantation embryogenesis and proliferation of primary embryonic fibroblasts. Bub1 inactivation in adult males inhibits proliferation in seminiferous tubules, reducing sperm production and causing infertility. In culture, Bub1-deficient fibroblasts fail to align their chromosomes or sustain SAC function, yielding a highly aberrant mitosis that prevents further cell divisions. Centromeres in Bub1-deficient cells also separate prematurely; however, we show that this is a consequence of SAC dysfunction rather than a direct role for Bub1 in protecting centromeric cohesion.

INTRODUCTION

The spindle assembly checkpoint (SAC) is an inhibitory signaling network that delays anaphase onset until all the chromosomes are stably attached to spindle microtubules via their kinetochores (Musacchio and Salmon, 2007). The SAC consists of "sensor" proteins such as Bub1, Mad1, and Mps1; a "signal transducer" known as the mitotic checkpoint complex (MCC), comprised of BubR1, Bub3, Mad2, and Cdc20; and an "effector," namely the anaphase promoting complex/ cyclosome (APC/C), a E3 ubiquitin ligase that targets anaphase inhibitors for proteolysis (Peters, 2006).

The SAC is not essential in budding yeast (Hoyt et al., 1991; Li and Murray, 1991), possibly because these cells enter mitosis with kinetochores already attached to microtubules (Gillett et al., 2004). By contrast, in vertebrate cells the SAC restrains normal mitotic progression (Taylor and McKeon, 1997; Gorbsky et al., 1998; Kops et al., 2004; Meraldi et al., 2004). Consistently, mice harboring homozygous null mutations in the MCC components Mad2, BubR1, and Bub3 die very early during embryogenesis (Dobles et al., 2000; Kalitsis et al., 2000; Babu et al., 2003; Wang et al., 2004). Likewise, ablation of *CENP-E* and *RAE1*, genes that encode a checkpoint-associated kinesin and a Bub3-related protein, respectively, also cause early embryonic lethality (Putkey et al., 2002; Babu et al., 2003).

Our understanding of the SAC in mammals has therefore largely been restricted to analysis of heterozygous mice harboring one null and one wild-type allele. Mouse embryo fibroblasts (MEFs) heterozygous for Mad2, BubR1, Bub3, Rae1, or Cenp-E all show SAC defects and increased levels of aneuploidy (Babu et al., 2003; Weaver et al., 2003; Dai et al., 2004; Burds et al., 2005; Kalitsis et al., 2005). Heterozygous animals develop normally but are predisposed to either spontaneous or carcinogen-induced tumors. Hypomorphic mice expressing ~11% BubR1 are not tumor prone but exhibit a premature aging phenotype, with isolated MEFs showing a penetrant SAC defect and high levels of aneuploidy (Baker et al., 2004). Bub3/Rae1 compound heterozygotes also age prematurely (Baker et al., 2006). These studies have been possible only because partial inhibition of MCC components yields penetrant effects on the SAC, consistent with the MCC being a stoichiometric inhibitor of the APC/C (Musacchio and Salmon, 2007). Indeed, reducing Mad2 protein levels to 70% totally abrogates the SAC in HCT-116 cells (Michel et al., 2001).

To define the role of the SAC sensor Bub1 in chromosome segregation, embryogenesis, and tissue homeostasis, we set out to mutate the murine *BUB1* gene. However, in contrast to MCC components, partial inhibition of Bub1 does not yield penetrant effects: HCT-116 cells heterozygous for *BUB1* are not haploinsufficent (V.L. Johnson & S.S.T., unpublished data), and RNAi-mediated repression of Bub1 has produced conflicting reports. While one study showed that Bub1 repression compromised the SAC (Meraldi and Sorger, 2005), others observed a premature loss of centromeric cohesion followed by SAC activation

(Tang et al., 2004; Kitajima et al., 2005). In our hands, Bub1 RNAi only yielded a penetrant SAC-defect when Aurora B activity was suppressed (Johnson et al., 2004; Morrow et al., 2005). Whether these differences reflect variations in repression levels and/or off-target RNAi effects is unclear. To avoid the ambiguities associated with partial loss-of-function phenotypes while also overcoming the problems associated with the early embryonic lethality typical of the SAC nulls described thus far, we used a *Cre-LoxP*-based approach to create a conditional null *BUB1* allele. Here, we demonstrate that Bub1 is essential not only for early embryogenesis but also later during development and for proliferation of MEFs in culture. By inactivating Bub1 in adult males, we also show that Bub1 is essential for spermatogenesis and fertility.

RESULTS

Generation of Conditional and Null BUB1 Alleles

Using homologous recombination in mouse ES cells, we flanked exons 7 and 8—which encode the Bub3 binding domain (Taylor et al., 1998)—with *LoxP* recombination sites to create the $BUB1^{F}$ allele (Figure 1A; see also the Supplemental Data available with this article online). Mice harboring this allele were then crossed with a Cre-deleter strain to create a null allele, $BUB1^{\Delta}$. Genotypes were confirmed by PCR and Southern blotting (Figures 1B, 1C, and 1D). While $BUB1^{F}$ could be bred to homozygosity (Figure 1C and 1D), breeding the $BUB1^{\Delta}$ allele to homozygosity resulted in embryonic lethality (see below). To confirm that $BUB1^{\Delta}$ was indeed a null, we prepared MEFs from 13.5-day $BUB1^{F/\Delta}$ embryos and transduced them with an adenovirus expressing Cre, thereby creating $BUB1^{\Delta/\Delta}$ cells. Western blotting showed that Bub1 protein was undetectable in $BUB1^{\Delta/\Delta}$ cells (Figure 1E). Blots probed with N-terminal antibodies failed to detect any truncation products in $BUB1^{\Delta/\Delta}$ cells (Figure S1), indicating that Bub1 coding sequence upstream of exon 6 is not expressed. These observations demonstrate therefore that $BUB1^{F}$ encodes a functional protein, that $BUB1^{\Delta}$ is indeed a null, and that *BUB1* is an essential gene.

Homozygous BUB1 Null Embryos Die Before Implantation

To determine when during development $BUB1^{\Delta/\Delta}$ animals died, we used a nested PCR assay capable of genotyping blastocysts and embryos cultured in vitro. While $BUB1^{\Delta/+}$ intercrosses failed to yield any $BUB1^{\Delta/\Delta}$ animals after day E8.5, they were present at day E3.5 (Figure 2A). When these blastocyst-stage embryos were grown in culture, they hatched and attached to the dish; but by day E10.5, only a few extraembryonic trophoblast cells were apparent, and there was no obvious inner cell mass (ICM, Figure 2B). By contrast, wild-type and $BUB1^{\Delta/+}$ blastocysts produced robust ICMs on a layer of trophoblasts. Confocal imaging of embryos cultured in vitro then fixed on day E7.5 and stained to detect phosphohistone H3 confirmed the presence of mitotic cells in the ICMs of control embryos but revealed no mitotic cells in the $BUB1^{\Delta/\Delta}$ cultures (Figure 2C). These observations confirm that $BUB1^{\Delta/\Delta}$ embryos die before implantation and are entirely consistent with the phenotypes exhibited by Mad2, Bub3, Cenp-E, Rae1, and BubR1 null embryos (Dobles et al., 2000; Kalitsis et al., 2000; Putkey et al., 2002; Babu et al., 2003; Wang et al., 2004).

Bub1 Is Required for Proliferation of Primary Embryonic Fibroblasts

To study the role of Bub1 at later stages of development, in adults, and in cultured cells, we crossed the Bub1 strains with mice harboring an ER^{T}-*Cre* transgene (Hayashi and McMahon, 2002). This transgene constitutively and ubiquitously expresses Cre fused to a mutated estrogen receptor, which responds to the artificial ligand 4-hydroxy-tamoxifen (OHT) rather than the endogenous ligand, estrogen. In the absence of OHT, the ER^{T}-Cre fusion protein is sequestered in the cytoplasm; upon binding of OHT, it translocates to the nucleus where it mediates recombination of genomic *LoxP* sites. Following OHT washout, the Cre-fusion returns to the cytoplasm thereby limiting any nonspecific genomic damage (Loonstra et al., 2001; Silver and Livingston, 2001). To validate the system, we isolated $BUB1^{F/+}$ and $BUB1^{F/\Delta}$ MEFs containing ER^{T}-*Cre* and exposed them in culture to OHT for 24 hr. PCR analysis of DNA from resulting cells showed very efficient conversion of $BUB1^{F}$ to $BUB1^{\Delta}$ (Figure 3A). Furthermore, western blotting demonstrated a dramatic reduction of Bub1 protein in OHT-treated $BUB1^{F/\Delta}$ cultures (Figure 3B); immunofluorescence analysis demonstrated that the majority of mitotic cells were completely devoid of kinetochore-bound Bub1 (Figure S2).

Having established that we could efficiently inactivate Bub1 in culture, we asked whether Bub1 was required for proliferation of primary embryonic fibroblasts. $BUB1^{F/+}$ and $BUB1^{F/\Delta}$ MEFs containing ER^{T}-*Cre* were plated at 80% confluency and cultured for 2 days to induce contact inhibition (Figure 3C). OHT was added for 48 hr in low serum to reinforce the growth arrest and promote cellular uptake of the OHT. On day 4, the OHT was removed, and the cultures expanded to alleviate the contact inhibition and trigger proliferation. Importantly, this synchronization regimen ensured that the cells did not progress into mitosis during the OHT treatment, thereby allowing us to study the first mitosis in the absence of Bub1. Untreated $BUB1^{F/\Delta}$ cultures proliferated normally (Figure 3D) and by day 8, 96 hr after release from the G1 block, they displayed DNA content profiles typical of proliferating cultures (Figure 3E). By contrast, treating $BUB1^{F/\Delta}$ cultures with OHT had a potent antiproliferative effect (Figure 3D); by day 8, the DNA content profiles had degenerated with many cells exhibiting sub-G1 and >4n DNA contents (Figure 3E); and the interphase nuclei were also highly distorted with abnormal lobes and micronuclei (Figure 3F), hallmarks of aberrant chromosome segregation. Although OHT treatment reduced Bub1 protein levels in $BUB1^{F/+}$ cultures (Figure 3B), due to inactivation of the *F* allele (Figure 3A), all the mitotic cells were Bub1-positive

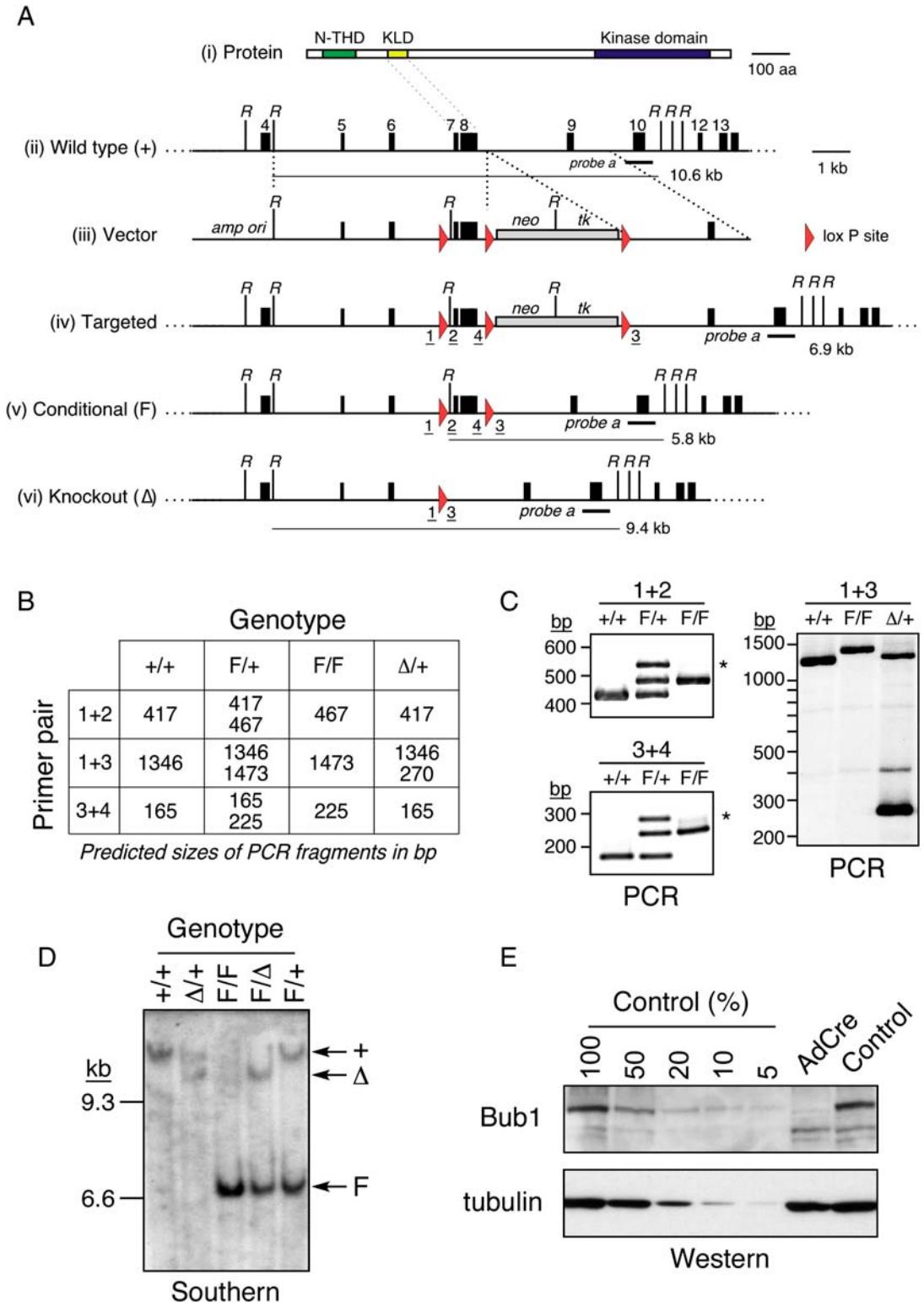

Figure 1. Creation of Conditional and Null BUB1 Alleles

(A) Schematic representations of (i) the Bub1 protein showing the N-terminal homology domain (N-THD), the Bub3-binding site/kinetochore localization domain (KLD), and the kinase domain; (ii) a portion of the *BUB1* gene showing exons 4–14 and the EcoRI restriction sites (R); (iii) the targeting vector showing the *neo-tk* cassette and *LoxP* sites; (iv) the structure of the correctly targeted allele; (v) the conditional allele (*F* for floxed); and (vi) the null allele (*Δ*). Also shown are the EcoRI restriction fragments detected by *probe a*. Underlined numbers show PCR genotyping primers 1–4.

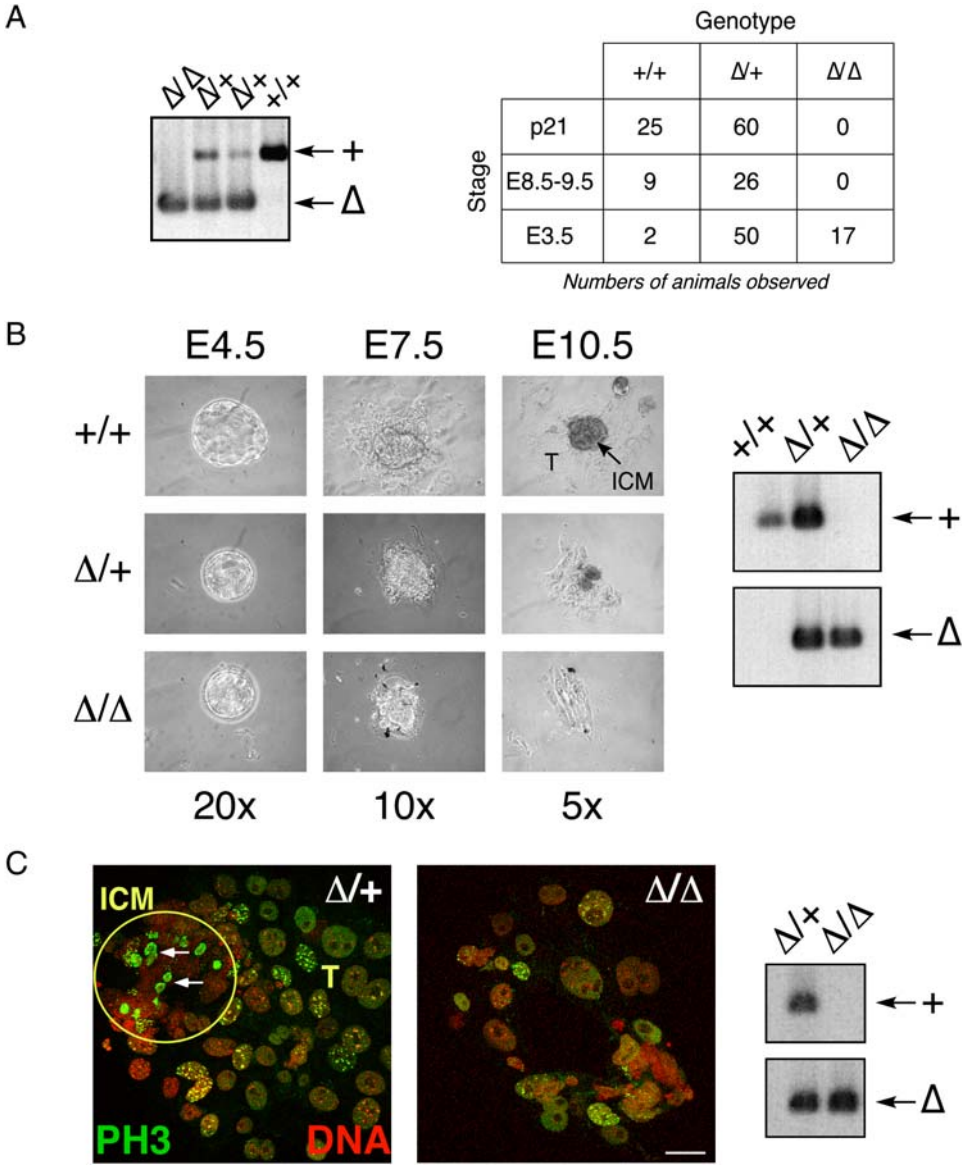

Figure 2. Embryonic Lethality of BUB1$^{\Delta/\Delta}$ Embryos

(A) PCR genotyping of blastocyst DNA using primers 1 and 2 and 1 and 3, confirming the presence of homozygous null embryos at day 3.5, plus a table showing the number of *BUB1*$^{\Delta/\Delta}$ animals observed at the age of weaning (p21), postimplantation (E8.5 to E9.5), and at the blastocyst stage (E3.5) following *BUB1*$^{\Delta/+}$ intercrosses.

(B) Phase contrast images of embryos harvested at day 3.5 and cultured in vitro for 7 days, plus PCR products obtained using primers 3 and 4 (upper panel) and 1 and 3 (lower panel) confirming the genotypes. Images, taken at progressively lower magnification, show that in contrast to Bub1 null embryos, the controls form a robust inner cell mass (ICM) upon a layer of trophoblast cells (T).

(C) Confocal images of embryos harvested at day 3.5 cultured in vitro for 4 days then fixed and stained to detect phospho-histone H3 (green) and the DNA (red), plus PCR genotypes obtained using primers 3 and 4 (upper panel) and 1 and 3 (lower panel). Arrows indicate examples of mitotic cells; note that cells in the *BUB1*$^{\Delta/\Delta}$ embryo which stain weakly for phospho-histone H3 are interphase cells. Scale bar, 50 μm.

due to the remaining wild-type allele (data not shown). Importantly, the OHT-treated *BUB1*$^{F/+}$ cultures proliferated normally (data not shown), confirming that OHT-mediated induction of Cre does not induce any overt toxicity and that inactivating one *BUB1* allele does not yield a penetrant haploinsufficient phenotype.

(B) Table showing the sizes of the PCR products generated by primers 1 and 2, 1 and 3, and 3 and 4 distinguishing the various genotypes.

(C) PCR products generated by amplifying tail snip DNA with the primers indicated. The asterisks indicate heteroduplexes formed by annealing of the larger and smaller PCR products.

(D) Southern blot of EcoRI-digested tail DNA probed with *probe a* confirming the genotypes.

(E) Western blots of *BUB1*$^{F/\Delta}$ MEFs infected with AdCre then probed to detect Bub1 and tubulin.

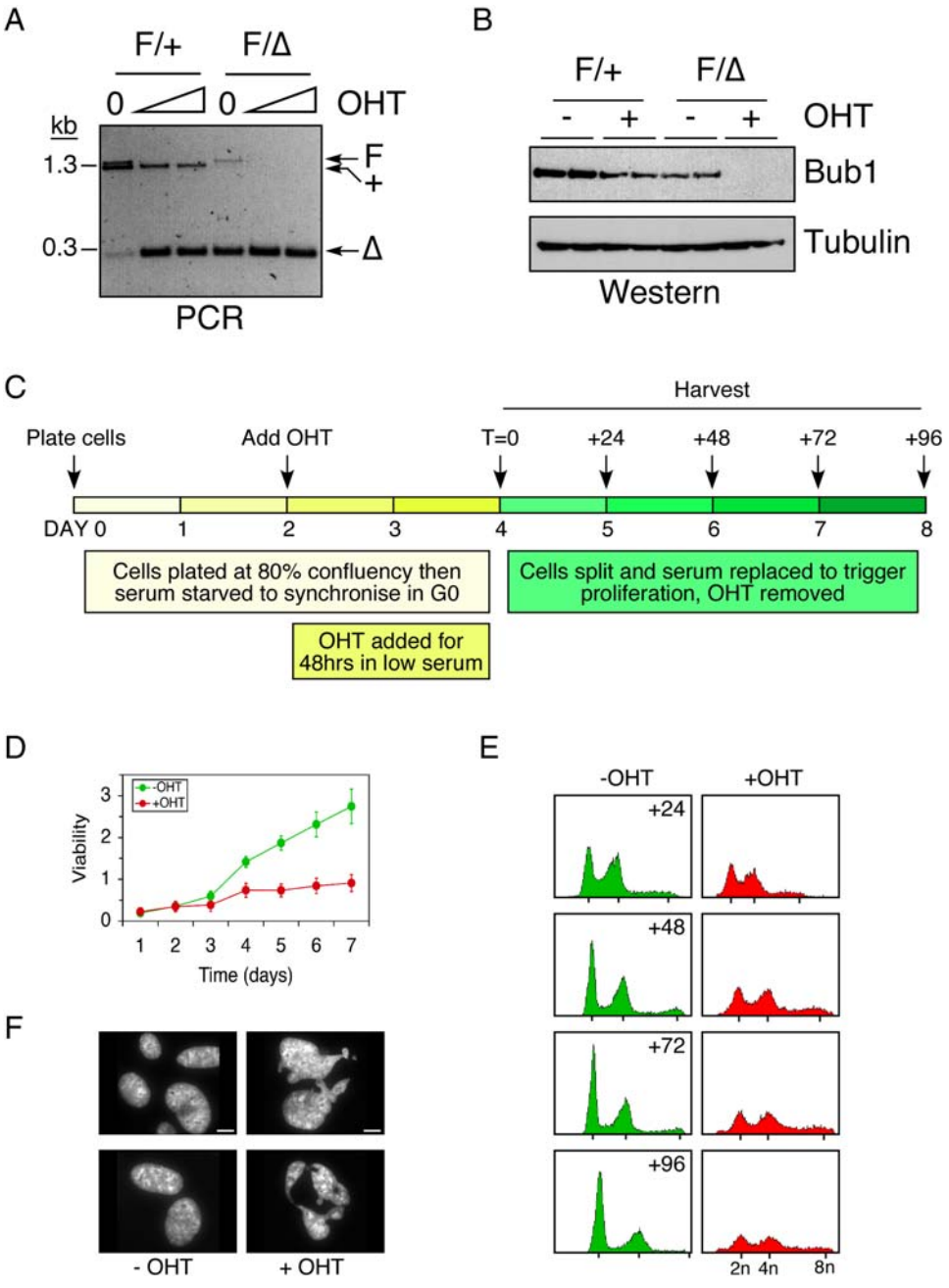

Figure 3. Tamoxifen-Induced Inactivation of Bub1 Inhibits Proliferation of Embryonic Fibroblasts

(A and B) *BUB1*$^{F/+}$ and *BUB1*$^{F/\Delta}$ MEFs harboring *ER*^{T}*-Cre* were treated with 0.1 and 1.0 μM OHT for 24 hr and then analyzed by PCR genotyping using primers 1 and 3 (A) and western blotting (B).

(C–F) *BUB1*$^{F/\Delta}$ *ER*^{T}*-Cre* MEFs were plated at 80% confluency, cultured for 2 days then treated with 0.1 OHT for 48 hr. On day 4 the cultures were expanded, the OHT removed, and the cells analyzed at subsequent time points. (C) Timeline showing experimental design. (D) Growth curves showing antiproliferative effect following Bub1-inactivation. (E) DNA content histograms showing marked reduction of cells with 2n and 4n values. (F) Fluorescence images of nuclei showing aberrant morphologies in Bub1 null cells.

Bub1 Is Required for Chromosome Alignment and SAC Function

Next, we analyzed the effect of Bub1-inactivation on SAC function and chromosome segregation. Previously, we showed that RNAi-mediated repression of Bub1 abolishes kinetochore localization of BubR1 (Johnson et al., 2004). This has since been challenged by others (Meraldi and Sorger, 2005). Therefore, we analyzed BubR1 in *BUB1*$^{F/\Delta}$ cells treated with OHT. Importantly, BubR1 protein levels were not affected following inactivation of Bub1 (Figure 4A). However, consistent with our previous observations, BubR1 did not localize to kinetochores in the

absence of Bub1 (Figure 4B). To define Bub1's requirement in SAC function, MEF cultures were challenged with the mitotic kinesin Eg5 inhibitor monastrol to prevent spindle assembly then analyzed by time-lapse microscopy. In the absence of monastrol, Bub1-proficient cells completed mitosis within ~1 hr (Figure 4C, −OHT −Mon). When challenged with monastrol, Bub1-proficient cells mounted a robust SAC response, delaying mitotic exit for on average ~3.5 hr (Figure 4C, −OHT +Mon). However, the vast majority of cells in the Bub1-deficient cultures exited mitosis within ~1 hr in both the presence and absence of monastrol (Figure 4C, +OHT ±Mon). Thus, while *BUB1* inactivation does not accelerate normal mitotic timing, it completely abolishes the SAC in response to monastrol. Similarly, inactivation of *BUB1* abrogated the SAC in MEFs exposed to the antitubulin agents, nocodazole and taxol (Figure S3).

To confirm that the SAC-defect was indeed due to inactivation of *BUB1*, we introduced a Myc-tagged Bub1 transgene into $BUB1^{\Delta/\Delta}$ cells using a recombinant adenovirus (Figure S4). While $BUB1^{\Delta/\Delta}$ cells infected with a control virus failed to mount a SAC response when challenged with monastrol, $BUB1^{\Delta/\Delta}$ cells infected with Bub1 viruses delayed mitotic exit by several hours (Figure 4D). Importantly, the ability of an exogenous Bub1 transgene to rescue the SAC defect in $BUB1^{\Delta/\Delta}$ cells confirms that the phenotype is indeed due to inactivation of *BUB1* rather than a nonspecific effect caused by exposure to OHT or activation of Cre. Note also that reconstituting Bub1 function in $BUB1^{\Delta/\Delta}$ cells restored BubR1 localization (Figure 4B), further confirming that Bub1 is required for kinetochore localization of BubR1.

Consistent with RNAi-based studies (Meraldi et al., 2004; Morrow et al., 2005), *BUB1* inactivation did not accelerate normal mitotic timing. This suggests that Bub1-deficient cells should have sufficient time to successfully align and segregate their chromosomes. Yet, in the absence of Bub1, proliferation is dramatically inhibited (Figure 3), suggesting that mitosis might be aberrant despite normal timing. To test this, we infected MEFs with a retrovirus encoding a GFP-tagged histone and then visualized chromosome movements by fluorescence time-lapse imaging. This revealed that chromosome segregation was highly aberrant in over 90% of the OHT-treated $BUB1^{F/\Delta}$ cells (Figure 4E, Table S1). Two phenotypes were prevalent: either the chromosomes decondensed without any obvious signs of chromosome alignment or anaphase movement, yielding a single large nucleus; or alternatively, the chromosomes moved poleward without forming a distinct metaphase plate, yielding lagging chromosomes, chromosome bridges, and distorted nuclei. Thus, despite normal mitotic timing, Bub1-deficient MEFs exit mitosis without correctly aligning their chromosomes.

Analysis of K-Fibers in Bub1-Deficient Cells

The lack of any apparent poleward movement in ~50% of $BUB1^{\Delta/\Delta}$ cells suggested a severe impairment of kinetochore-microtubule interactions. Therefore, to ascertain whether kinetochore fibers (K-fibers) form, $BUB1^{F/\Delta}$ cells treated with OHT were exposed to the proteasome inhibitor MG132 for 1 hr to arrest mitotic cells in metaphase. The cells were then fixed to selectively preserve K-fibers and stained to detect microtubules and chromosomes (Figure 5A). We also stained for Bub1 (data not shown) to ensure that the OHT-treated cells were indeed Bub1-deficient. In control cells, perfect metaphases were readily apparent with all the chromosomes aligned at the spindle equator; closer inspection revealed bioriented chromosomes (Figure 5A). In Bub1-deficient cells, metaphases were apparent, but they appeared more disorganized; the metaphase plate appeared broader with some chromosomes clustered near the spindle poles (Figure 5A). Consistent with the majority of chromosomes being able to align, K-fibers were readily apparent indicating that kinetochore-microtubule interactions are not completely inhibited in Bub1-deficient cells. Note that K-fibers were also apparent in the absence of MG132 (data not shown).

Bub1 Maintains Sister Chromatid Cohesion by Activation of the Spindle Checkpoint

The chromosome segregation failure in $BUB1^{\Delta/\Delta}$ cells could also be explained by a premature centromere separation (PCS) due to a centromeric cohesion defect (Tang et al., 2004; Kitajima et al., 2005). To ascertain the status of centromeric cohesion in the absence of Bub1, we treated $BUB1^{F/\Delta}$ MEFs with OHT, added nocodazole, then prepared chromosome spreads. In controls, all the chromosomes in 100% of the spreads had cohesed centromeres (Figure 5B, panels i and iv, n = 278). Treatment of controls with okadaic acid, a PP2A inhibitor, induced PCS in ~56% of the cells (Figure 5B, panel vi, n = 27), consistent with observations demonstrating that PP2A sustains centromeric cohesion by targeting Sgo1 to centromeres (Kitajima et al., 2006; Riedel et al., 2006; Tang et al., 2006). In $BUB1^{F/\Delta}$ MEFs treated with OHT, the vast majority of chromosome spreads had cohesed centromeres; PCS was obvious in only ~11% of the cells (Figure 5B panels ii and iii, n = 178). In the example shown in Figure 5B, panel iii, all the sister centromeres appeared to be separated, as one would expect in a cell that had committed to anaphase, i.e., switched off the SAC, activated the APC/C, and degraded securin. Because these MEFs require Bub1 for SAC function (Figure 4), we reasoned that the PCS could be due to SAC override rather than a direct effect on Sgo1-dependent protection of centromeric cohesion (Tang et al., 2004; Kitajima et al., 2005). To test this, we treated the MEFs with MG132 during the nocodazole block. We predicted that if Bub1 maintained cohesion by inhibiting securin proteolysis via APC/C-inhibition, then in the presence of MG132, sisters should remain cohesed due to the inability to degrade securin. If by contrast Bub1 plays a direct role in protecting centromeric cohesion independent of its role in the SAC, e.g., via Sgo1 targeting, then inhibiting proteolysis would have no effect and the centromeres should separate prematurely. Significantly, in the presence of MG132, we observed no PCS in OHT-treated $BUB1^{F/\Delta}$ MEFs; under

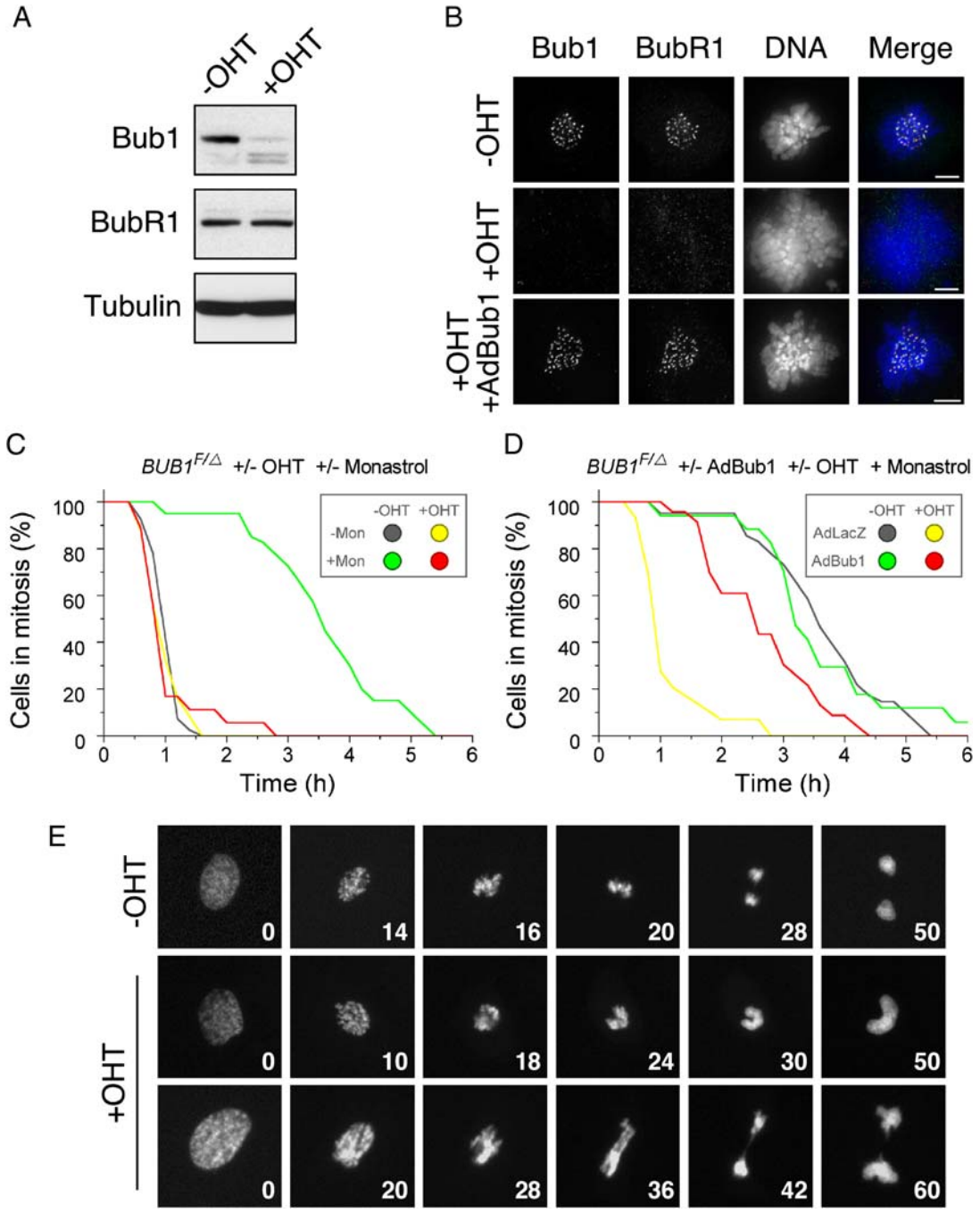

Figure 4. Bub1 Is Required for Kinetochore Targeting of BubR1 and SAC Function

Asynchronous *BUB1*$^{F/\Delta}$ *ER*^{T}*-Cre* MEFs were treated with 0.5 μM OHT for 24 hr then analyzed by western blotting, immunofluorescence, and time-lapse microscopy. In (B) and (D), cells were preinfected with adenoviral vectors as indicated. In (E), cells were preinfected with retrovirus encoding a GFP-tagged histone H2B.

(A) Western blots showing that BubR1 levels are unaffected following Bub1 inactivation. Tubulin was used as loading control.

(B) Projections of deconvolved image stacks showing that kinetochore localization of BubR1 requires Bub1. Scale bar, 5 μm.

(C and D) Line graphs plotting the percentage of cells in mitosis in the presence or absence of monastrol as indicated. The time in mitosis is defined as the interval between nuclear envelope breakdown and chromosome decondensation, as determined by phase-contrast time-lapse analysis. At least 18 cells were analyzed in each condition.

(E) Fluorescence images from time-lapse sequences. Numbers represent minutes after NEBD.

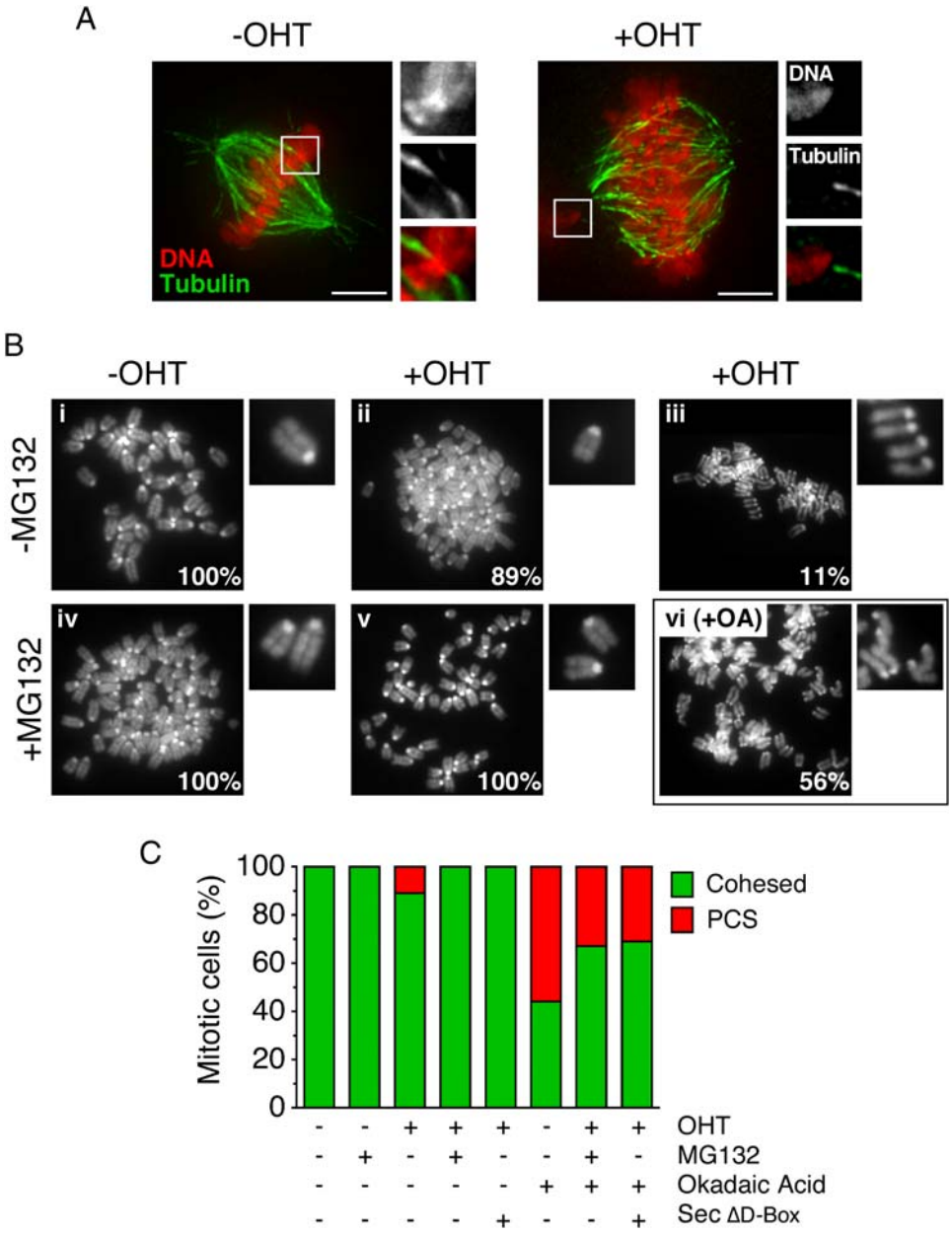

Figure 5. K-Fibers Form and Centromeric Cohesion Is Maintained in Bub1 Null Cells

(A) *BUB1*$^{F/\Delta}$ *ER*^{T}*-Cre* MEFs were synchronized and exposed to 0.1 μM OHT as shown in Figure 3C. At T = 24 hr, the cells were treated with MG132 for 1 hr to arrest the cells downstream of the SAC, fixed to preserve K-fibers, and then stained to detect tubulin (green), Bub1 (not shown), and DNA (red). Images show projections of deconvolved image stacks. Enlargement shows a mono-oriented chromosome in the Bub1 null cell. Scale bar, 5 μm.

(B) Asynchronous *BUB1*$^{F/\Delta}$ *ER*^{T}*-Cre* MEFs were treated with 0.5 μM OHT for 24 hr, exposed to nocodazole ± MG132 for 1 hr then chromosome spreads prepared and scored for premature centromere separation (PCS). As a positive control, cells were treated with okadaic acid. Images and enlargements show examples of spreads and individual chromosomes respectively. Percentages show the number of spreads represented by that image.

(C) Bar graph quantitating the percentage of mitotic cells exhibiting PCS.

these conditions, all the chromosomes in 100% of the spreads analyzed had cohesed centromeres (Figure 5B, panel v, n = 150). Furthermore, overexpression of a non-degradable securin also prevented PCS in *BUB1*$^{\Delta/\Delta}$ MEFs, confirming that Bub1 maintains centromeric cohesion by activation of the SAC (Figure 5C).

Tamoxifen-Induced Inactivation of Bub1 in Adult Males Causes Infertility

Having established that OHT-mediated induction of Cre efficiently inactivated Bub1 in *BUB1*$^{F/\Delta}$ MEFs, we asked whether this approach could inactivate Bub1 in adult mice. Interestingly, in contrast to Bub3, Bub1 was only

detectable in the testes of wild-type adults (Figure S5); therefore, we focused on this particular tissue. *BUB1*$^{F/F}$ males were injected with tamoxifen dissolved in corn oil, and, as controls, we injected *BUB1*$^{F/F}$ males with corn oil alone. In addition, we injected *BUB1*$^{F/+}$ males with either tamoxifen or corn oil (Table S2). Each male was injected weekly for four consecutive weeks. To test fertility, each male was housed with two wild-type females during weeks 3 and 4. Although all the females presented vaginal plugs after mating, no litters were obtained from matings involving *BUB1*$^{F/F}$ males injected with tamoxifen (Table S2). By contrast, *BUB1*$^{F/F}$ males injected with corn oil, or *BUB1*$^{F/+}$ males injected with either tamoxifen or corn oil, all yielded litters. (Females that did not yield litters were then mated with fertile males, confirming female fertility.) The infertile males—which presented no overt phenotype after 4 weeks of treatment—were then sacrificed and the testes analyzed. PCR genotyping confirmed efficient conversion of the *F* alleles to *Δ* (Figure 6A), while western blotting demonstrated ablation of Bub1 protein in both *BUB1*$^{F/\Delta}$ and *BUB1*$^{F/F}$ animals (Figure 6B).

To determine the cause of infertility, *BUB1*$^{F/F}$ males were injected with tamoxifen every week for 8 weeks and the testes then analyzed. Histological sections of Bub1-deficient testis revealed major abnormalities, including decreased cellularity and reduced diameter of the tubules (Figure 6C). Tubules containing only Sertoli cells were frequently observed, indicating that proliferation of the spermatogonia was inhibited and that germ cells were no longer produced. As a consequence of major alterations in the composition of the germ cell layer, staging of the tubules in Bub1-deficient testis sections was frequently impossible (Figure 6D). Furthermore, clusters of M-phase cells and tubules with mature sperm cells were less apparent following Bub1 inactivation (Figure S6, Table S3). Where mitotic clusters were observed in Bub1-deficient testes, abnormal anaphases were often apparent (Figure 6D and Figure S6). Spermatocytes with abnormal chromosome contents were also apparent (Figure S6). Consistent with this dramatic effect, the weight of Bub1-deficient testis was reduced by ~50% (Figure S6), and sperm production was reduced by over 80% (Figure S7). Thus, inactivation of Bub1 in adult males impairs normal chromosome segregation and inhibits spermatogenesis, resulting in infertility.

Bub1 Is Required for Postimplantation Development

Despite being infertile, *BUB1*$^{F/F}$ *ER*^{T}*-Cre* males injected with tamoxifen appeared largely normal. Although Cre-mediated recombination was observed in tissues other than testes (data not shown), it may have been less efficient, leading to only partial inactivation of Bub1. Alternatively, in contrast to the testes, most tissues in adult mice consist of nondividing cells; these tissues may therefore be less sensitive to Bub1-inactivation. Indeed, while we could detect Bub3 in a variety of tissues, Bub1 was only detectable in the testes (Figure S5). Therefore, to investigate the effect of inactivating Bub1 in tissues containing a higher proportion of proliferating cells, we inactivated Bub1 in postimplantation embryos by injecting tamoxifen into pregnant females. Timed matings were set up between *BUB1*$^{F/F}$ males and *BUB1*$^{\Delta/+}$ females harboring *ER*^{T}*-Cre* (Figure 7A). The advantage of this mating regimen was two-fold. First, the resulting embryos would be either *BUB1*$^{F/\Delta}$ or *BUB1*$^{F/+}$, in roughly equal proportions, and harbor *ER*^{T}*-Cre*. Second, because the female lacks *F* alleles, tamoxifen-mediated induction of Cre should have no effect in the pregnant host. Ten and a half days post coitum (p.c.), the female was injected with tamoxifen, then 18.5 days p.c., the embryos were harvested and genotyped, identifying five *BUB1*$^{F/+}$ and four *BUB1*$^{F/\Delta}$ embryos (Figure 7B). While the *BUB1*$^{F/+}$ embryos appeared as one would expect for 18.5 day embryos, i.e., completely normal, the *BUB1*$^{F/\Delta}$ embryos were clearly abnormal (Figure 7C). Specifically, in both size and shape they appeared similar to embryos normally found at day E10.5–E11.5 (Nagy et al., 2003). Whether these developmentally arrested embryos were alive or dead at day 18.5 is unclear; indeed, we were surprised that the abnormal embryos were not resorbed. Defining which cells express Bub1 during embryogenesis, the frequency of *BUB1* inactivation and the cause of the developmental arrest will require further analysis.

DISCUSSION

Here we describe, for the first time, the phenotype of mammalian cells, tissues, and embryos rendered homozygous null for Bub1. We show that Bub1 is essential for early embryogenesis, with *BUB1*$^{\Delta/\Delta}$ animals dying between day E3.5 and E8.5. Lethality at this time, which occurs in all homozygous SAC mutants examined to date (Dobles et al., 2000; Kalitsis et al., 2000; Putkey et al., 2002; Babu et al., 2003; Wang et al., 2004; Iwanaga et al., 2007), may reflect the very rapid cell divisions that occur in the early embryo (Nagy et al., 2003). To overcome early embryonic lethality, we used a *Cre-LoxP*-based approach to inactivate Bub1 at later developmental stages. Tamoxifen-induced gene ablation in postimplantation embryos shows that Bub1 is also essential following gastrulation and the initiation of organogenesis: day 10.5 embryos arrest development shortly after Bub1 inactivation. Bub1 is also required for proliferation of primary embryonic fibroblasts isolated at day E13.5. In the absence of Bub1, MEFs undergo one highly aberrant mitosis, but the marked reduction in cell number, plus the paucity of mitotic cells at later time points, suggests that they do not divide again. The ability to inactivate Bub1 by small molecule exposure has also allowed us to study Bub1 function in adult tissues. Tamoxifen-induced inactivation of Bub1 occurred very efficiently in the testes, resulting in infertility. Consistent with the antiproliferative effect observed in embryos and cultured MEFs, phosphohistone-H3-positive cells and mature spermatids were less apparent in Bub1-deficient seminiferous tubules. Thus, in the four different scenarios we have examined, Bub1 is essential for cellular proliferation.

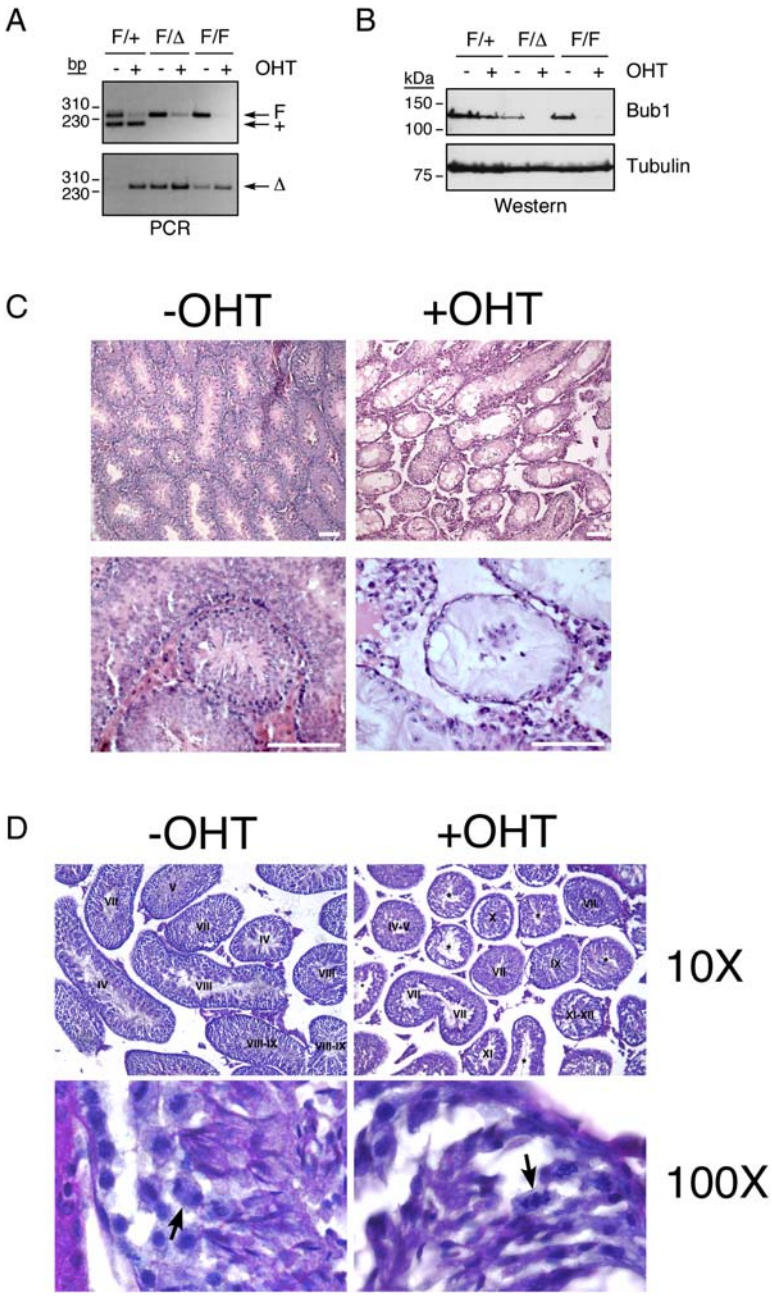

Figure 6. Bub1 Is Required for Spermatogenesis

Male mice harboring conditional Bub1 alleles and the *ER^T-Cre* transgene were injected with tamoxifen, and the testes were isolated and analyzed by PCR genotyping, western blotting, and histology.

(A) PCR genotyping with primers 3 and 4 (upper panel) and 1 and 3 (lower panel) demonstrating efficient conversion of *F* alleles to *Δ*.

(B) Western blot confirming depletion of Bub1 protein in *BUB1$^{F/Δ}$* and *BUB1$^{F/F}$* males following tamoxifen exposure.

(C) Hematoxylin/eosin-stained testes sections showing aberrant tubule morphology in Bub1-deficient testes. Scale bar, 100 μm.

(D) PAS/hematoxylin-stained tubules showing that following tamoxifen treatment, tubules are frequently abnormal and often cannot be staged (asterisks). Roman numerals indicate tubules in various stages of spermatogenesis, arrows indicate anaphases.

We also examined the effect of Bub1-inactivation on chromosome segregation and SAC function. These issues have previously been addressed by several RNAi-based studies in HeLa cells, yielding conflicting reports. In two studies, Bub1-repression induced Sgo1 mislocalization and premature centromere separation, which in turn activated the SAC (Tang et al., 2004; Kitajima et al., 2005). In our hands, repressing Bub1 by ~98% was not sufficient to prevent mitotic arrest in response to spindle damage (Johnson et al., 2004; Morrow et al., 2005). A fourth study repressed Bub1 by ~99.5% which was sufficient to override the SAC (Meraldi and Sorger, 2005); however, despite more extensive repression in this latter study, BubR1 localized to kinetochores depleted of Bub1, an observation which is inconsistent with our previous analysis (Johnson et al., 2004). Our new data derived from Bub1 null MEFs clarifies these issues. We confirm our earlier observation that Bub1 is indeed required to target BubR1 to kinetochores. In addition, we show that Bub1 is required to prevent anaphase onset in the presence of unaligned chromosomes and mitotic exit when spindle assembly is compromised.

We also observed premature centromere separation in Bub1 null cells. However, having unambiguously demonstrated that Bub1 is required for SAC function, we were concerned that this might be due to SAC-override rather

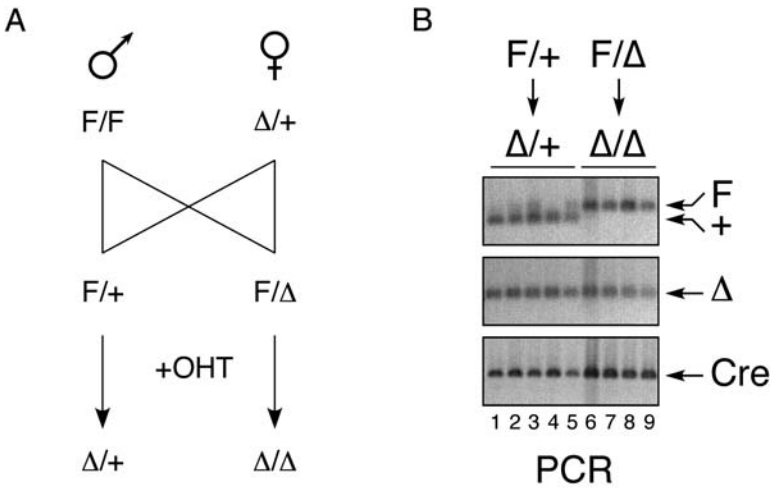

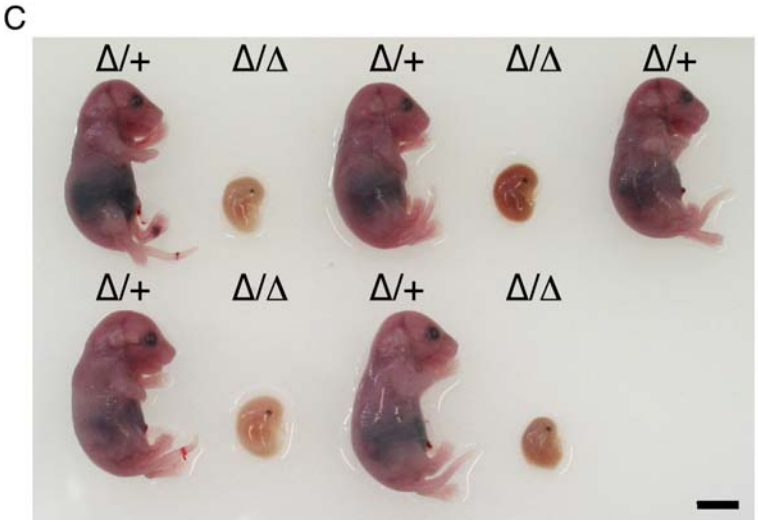

Figure 7. Bub1 Is Required for Postimplantation Embryo Development

A *BUB1$^{F/F}$ ER^{T}-Cre* male was crossed with a *BUB1$^{Δ/+}$ ER^{T}-Cre* female. Ten and a half days p.c., the female was injected with tamoxifen and then on day 18.5 p.c., the embryos were harvested and genotyped.

(A) Schematic of mating regimen.

(B) PCR genotyping using primers 3 and 4 (upper panel) and 1 and 3 (middle panel) to confirm the genotype and the presence of *Cre* (lower panel). Note that recombination is not 100% efficient, explaining the presence of *F* alleles in tamoxifen-treated *BUB1$^{F/Δ}$* embryos.

(C) Images of embryos shortly after harvesting on day 18.5 showing arrested development in the *BUB1$^{F/Δ}$* animals. Scale bar, 5 mm. The genotypes of the *F*/+ and *F*/*Δ* embryos are shown in lanes 1–5 and 6–9, respectively, in panel B.

than a direct effect on Sgo1-mediated protection of centromeric cohesion (Tang et al., 2004; Kitajima et al., 2005). Indeed, when we inhibited the proteasome or expressed a nondegradable securin to prevent activation of separase in Bub1-deficient cells, sister centromeres remained cohesed. This is inconsistent with the notion that Bub1 protects centromeres from the "prophase pathway" which removes cohesin from chromosome arms in a separase-independent manner (Tang et al., 2004; Kitajima et al., 2005). Interestingly, an anti-Sgo1 antibody (Tang et al., 2004) decorates kinetochores in MEFs, and this is abolished upon Bub1 deletion (Figure S8). However, this antibody detects several bands on MEF western blots (data not shown), so we cannot be certain which Sgo1 isoform localizes to mouse kinetochores in a Bub1-dependent manner. Nevertheless, despite the mislocalization of this Sgo1 isoform, centromeric cohesion is maintained when proteolysis is inhibited. How can we explain these inconsistencies? First, in the absence of an obvious SAC defect, the observed centromere separation might not have been considered to be a manifestation of SAC dysfunction; the effect of MG132 on centromere separation was not reported in the Bub1 RNAi studies (Tang et al., 2004; Kitajima et al., 2005). Second, the differences may reflect differences between primary mouse fibroblasts and transformed human, epithelial-derived cells. Third, the functional roles of Sgo-related proteins do not appear to be restricted to protecting centromeric cohesion; Sgo2 has recently been shown to play a role in regulating components of the chromosome passenger complex (CPC) (Salic et al., 2004; Huang et al., 2007; Kawashima et al., 2007; Vanoosthuyse et al., 2007). Finally, because components of the RNAi machinery are required for centromeric heterochromatin structure (Fukagawa et al., 2004), RNAi-mediated repression of centromere/kinetochore proteins may result in synthetic interactions that disrupt centromeric cohesion.

Despite the fact that all the homozygous null SAC mutants described to date result in embryonic lethality, it was recently suggested that the SAC is not essential in mammals (Burds et al., 2005). This was based on the

isolation of Mad2 null lines from E10.5 *MAD2*$^{-/-}$/*p53*$^{-/-}$ mice (Burds et al., 2005). Note, however, that these lines are p53 deficient and arise infrequently; culturing 208 embryos yielded only two lines. Furthermore, although Mad2 loss overrides the SAC and accelerates mitotic timing, ~45% of these cells separate their chromosomes normally, and ~30% divide with only a single lagging chromosome, possibly explaining why these cells can give rise to viable lines. By contrast, the effect of inactivating Bub1 is very different; chromosome segregation is disastrous in Bub1 null cells despite no obvious effect on mitotic timing. Consistently, Bub1 is essential, not only in cultured primary fibroblasts but also in very early embryos, day 10.5 embryos, and during transmission of the male germline. Indeed, in contrast to Mad2, Bub1's function extends beyond the SAC. A role for Bub1 in chromosome congression—independent of its SAC function—has been alluded to in yeast (Bernard et al., 1998; Warren et al., 2002; Kitajima et al., 2004). We showed that RNAi-mediated repression of Bub1 inhibits chromosome congression in HeLa cells (Johnson et al., 2004), an observation later confirmed by others (Meraldi and Sorger, 2005). In this latter case, increased lateral and syntelic orientations were observed, mal-orientations typically observed following CPC inhibition. It is possible therefore that, in contrast to the MCC components, depletion of the checkpoint sensor Bub1 not only negates the SAC but also inhibits CPC activity, possibly by compromising Shugoshin function, and thereby inhibiting chromosome biorientation.

In summary, we show here that, in contrast to the other SAC mutants described so far, mitosis is disastrous in *BUB1*$^{\Delta/\Delta}$ cells due to a failure in both chromosome alignment and SAC function, resulting in potent antiproliferative effects in culture, during embryogenesis, and in adult tissues. By contrast, heterozygous *BUB1* animals and MEFs did not exhibit any overt abnormalities. This is consistent with the lack of penetrant effects in RNAi-based experiments (Johnson et al., 2004; Morrow et al., 2005), highlighting the limitation of RNAi when studying protein kinases which concentrate at discrete subcellular localizations. The conditional *BUB1* strain described here has not only allowed us to generate bona fide Bub1 null cells, but by introducing a tamoxifen-inducible Cre, we have avoided the early embryonic lethality exhibited by all of the SAC mutant mice described thus far. This system will now allow us to further explore the role of Bub1 in development, tissue homeostasis, tumorigenesis, and aging.

EXPERIMENTAL PROCEDURES

Construction of Mouse Strains

A mouse genomic library was screened with an mBub1 cDNA fragment (Taylor and McKeon, 1997), and the isolated clones were then mapped and sequenced. To generate the targeting vector, fragments containing exons 5–8 and 9 were cloned into a pKO-derived vector (Stratagene) (Figure 1A). A *LoxP* site was engineered upstream of exon 7, and a *LoxP-neo-tk-LoxP* cassette was then inserted downstream of exon 8. The construct was linearized and electroporated into ES cells; Southern blotting with *probe a* (Figure 1A) was then used to identify correctly targeted clones. The *neo-tk* cassette was then removed by transient transfection of Cre. *BUB1*$^{F/+}$ ES cells were injected into C57BL/6J blastocysts to generate *BUB1*$^{F/+}$ animals. *BUB1*$^{F/+}$ mice were crossed with a deleter *Cre* line to create the *Δ* allele. To distinguish between the different alleles, tail snip DNA was PCR genotyped using primers 1, 2, 3, and 4 (Figures 1A and 1B and Table S4). The *ER*^{T}*-Cre* transgenic line was obtained from Jackson Laboratories (Bar Harbor, USA), and the presence of the transgene was confirmed by PCR (Table S4). All mice were hosted in a pathogen-free facility at the University of Manchester. For more details see the Supplemental Data.

Isolation and Culture of Embryos and Mouse Embryo Fibroblasts

Three and a half day embryos were isolated from superovulated females, placed in gelatin-coated plates, and cultured in DMEM plus 15% fetal calf serum, 100 U/ml penicillin, 100 μg/ml streptomycin, and 2 mM glutamine (Invitrogen). To genotype blastocysts and in vitro embryo cultures, nested PCR was performed using primers 1′, 2′, 3′, and 4′ (Table S4) followed by primers 1–4 as described above. MEFs from 13.5 d embryos were prepared using standard procedures (Nagy et al., 2003), then cultured in gelatin-coated flasks as above but in 10% serum and 3% oxygen. To induce Cre, MEFs were cultured in optiMEM media (Invitrogen) plus 2% charcoal/dextran-treated serum (Hyclone); 4-hydroxy-tamoxifen (Sigma, 10 mg/ml stock in ethanol) was added at 0.1 or 0.5 μM. Nocodazole, taxol, and MG132 were used at final concentrations of 0.2 μg/ml, 10 μM, and 20 μM, respectively. Okadaic acid (Calbiochem) and monastrol (Sigma) were used at final concentrations of 10 μM and 100 μM, respectively.

Cell Biology

For western blotting, proteins were extracted in lysis buffer (10 mM Tris pH 7.4, 100 mM NaCl, 1 mM EDTA, 1 mM EGTA, 0.1% Triton X-100, 10 mM β-glycerophosphate, 1 mM DTT, 0.2 mM PMSF, and protease inhibitors), transferred to nitrocellulose membranes, blocked in TBST (50 mM Tris, pH 7.6, 150 mM NaCl, 0.1% Tween-20) plus 5% nonfat dried milk, and probed with the following antibodies: SB1.3 (sheep anti-Bub1, 1:1,000 [Taylor et al., 2001]), SBR1.1 (sheep anti-BubR1, 1:1,000, [Taylor et al., 2001]), and TAT1 (mouse anti-tubulin, 1:5,000, gift from Keith Gull, Oxford). For immunofluorescence analysis, cells and embryos were fixed in PBS plus 1% formaldehyde, permeabilized in 0.1% Triton X-100, and then stained with the following primary antibodies: 4B12 (mouse anti-Bub1, 1:10, [Taylor and McKeon, 1997]), SBR1.1 (1:100), TAT1 (1:200), and rabbit anti-phospho-histone H3 (serine 10, 1:200, Upstate Biotechnology). To preserve K-fibers, cells were permeabilized for 90 s in K-buffer (100 mM PIPES pH 6.8, 1 mM MgCl, 0.1 mM $CaCl_2$, 0.1% Triton X-100) at room temperature, fixed for 10 min in 4% formaldehyde diluted in K-buffer, and then processed as above. Widefield microscopy, deconvolution, and imaging processing were all done as described (Taylor et al., 2001). Confocal imaging of embryos was performed using a Leica SP2 AOBS microscope. To prepare chromosome spreads, MEFs were treated with nocodazole for 5 hr, incubated in hypotonic buffer for 30 min, then fixed in fresh Carnoy's solution (methanol/acetic acid, 3:1). Chromosomes were spread on glass slides, air-dried, and stained with Hoechst 33358 (Sigma). Flow cytometry was done as described (Taylor et al., 2001) using a Cyan (DakoCytomation). Growth curves using the crystal violet method were as described (Hussein and Taylor, 2002). Time-lapse microscopy was done as described previously (Morrow et al., 2005), acquiring images every 2 minutes. XY point visiting was performed using a PZ-2000 automated stage (Applied Scientific Instrumentation).

Viral Infections

The adenovirus expressing Cre was purchased from Microbix Biosystems, Inc. (Canada). Recombinant adenoviruses expressing a Myc-tagged mBub1 transgene were generated using the AdEasy system (Stratagene) according to the manufacturer's instructions. MEF cultures were infected with an MOI of ~100, with LacZ viruses serving

as a negative control. For retroviral infections, cDNAs encoding a GFP-tagged histone H2B (Morrow et al., 2005) or a Myc-tagged securin D-box/KEN box double mutant (Hagting et al., 2002) were cloned into a pLPCX-based vector (Hussein and Taylor, 2002). The resulting plasmids were transfected into Phoenix-Eco packaging cells (kindly provided by Gary Nolan, Stanford) using the calcium phosphate method. Subconfluent cultures were incubated overnight in the absence of serum, the viral supernatant harvested, passed through a 0.2 μm filter, and $CaCl_2$ and polybrene added to final concentrations of 4 mM and 4 μg/ml, respectively. Viruses were then added to MEFs for 24 hr.

In Vivo Inactivation of Bub1

Adult males were injected (i.p.) once a week for 4 or 8 weeks with tamoxifen (Sigma, 5 mg per 40 g body weight) dissolved in corn oil (Sigma). For western blotting, the outer capsule was removed from one testis, and the remaining tissue was finely chopped and washed with PBS. Samples were lysed with 6 M urea, 1% SDS, 0.1% β-mercaptoethanol, and 20 mM Tris pH 6.8; sonicated and centrifuged for 5 min at 13,000 rpm; and the supernatants collected for analysis. Protein samples were subjected to SDS-PAGE and then transferred to nitrocellulose. For histological analysis, testes and epididymides were dissected and fixed in Bouin's solution. Paraffin sections (5 μm) were deparaffinized, rehydrated, and stained with periodic acid Schiff (PAS)/hematoxylin or hematoxylin/eosin. For the detection of sperm in epididymides, sections were stained with Hoechst 33358. For detection of phospho-histone H3, sections were blocked in PBS plus 5% BSA, then stained with rabbit anti-phospho-histone H3 antibody (1:50) overnight at 4°C. Following washes in PBS, sections were stained with an Alexa488-labeled secondary antibody (Molecular Probes) diluted 1:500, stained with Hoechst 33358, and then mounted. Following timed matings, pregnant females were injected (i.p.) at 10.5 days p.c. with tamoxifen (5 mg per 40 g body weight) dissolved in corn oil and then sacrificed on day 18.5. The animal studies were carried out according to Home Office and Institutional guidelines.

Supplemental Data

The Supplemental Data include seven figures, two tables, and Supplemental Experimental Procedures and can be found with this article online at http://www.developmentalcell.com/cgi/content/full/13/4/566/DC1/.

ACKNOWLEDGMENTS

The authors thank Chitra Chakravarthy, Silke Warnke, Eamon Dubaissi, and BSF staff for technical assistance. We thank Janni Petersen, Andrew Holland, Mailys Vergnolle, Phil Woodman, and Charles Streuli for comments on the manuscript. J.A.H. was funded by a project grant from Cancer Research UK; M.B. was funded by "Rientro dei Cervelli 2005," MIUR, Italy; D.P., V.T., and S.S.T. are funded by a Senior Fellowship from Cancer Research UK. The project was conceived and managed by S.S.T; the conditional *BUB1* strain was created by J.A.H. with advice and technical assistance from R.B.H.; and experiments described here were performed by D.P., V.T., and M.B. The manuscript was written by S.S.T.

Received: March 28, 2007
Revised: July 31, 2007
Accepted: August 16, 2007
Published: October 9, 2007

REFERENCES

Babu, J.R., Jeganathan, K.B., Baker, D.J., Wu, X., Kang-Decker, N., and van Deursen, J.M. (2003). Rae1 is an essential mitotic checkpoint regulator that cooperates with Bub3 to prevent chromosome missegregation. J. Cell Biol. *160*, 341–353.

Baker, D.J., Jeganathan, K.B., Cameron, J.D., Thompson, M., Juneja, S., Kopecka, A., Kumar, R., Jenkins, R.B., de Groen, P.C., Roche, P., and van Deursen, J.M. (2004). BubR1 insufficiency causes early onset of aging-associated phenotypes and infertility in mice. Nat. Genet. *36*, 744–749.

Baker, D.J., Jeganathan, K.B., Malureanu, L., Perez-Terzic, C., Terzic, A., and van Deursen, J.M. (2006). Early aging-associated phenotypes in Bub3/Rae1 haploinsufficient mice. J. Cell Biol. *172*, 529–540.

Bernard, P., Hardwick, K., and Javerzat, J.P. (1998). Fission yeast bub1 is a mitotic centromere protein essential for the spindle checkpoint and the preservation of correct ploidy through mitosis. J. Cell Biol. *143*, 1775–1787.

Burds, A.A., Lutum, A.S., and Sorger, P.K. (2005). Generating chromosome instability through the simultaneous deletion of Mad2 and p53. Proc. Natl. Acad. Sci. USA *102*, 11296–11301.

Dai, W., Wang, Q., Liu, T., Swamy, M., Fang, Y., Xie, S., Mahmood, R., Yang, Y.M., Xu, M., and Rao, C.V. (2004). Slippage of mitotic arrest and enhanced tumor development in mice with BubR1 haploinsufficiency. Cancer Res. *64*, 440–445.

Dobles, M., Liberal, V., Scott, M.L., Benezra, R., and Sorger, P.K. (2000). Chromosome missegregation and apoptosis in mice lacking the mitotic checkpoint protein Mad2. Cell *101*, 635–645.

Fukagawa, T., Nogami, M., Yoshikawa, M., Ikeno, M., Okazaki, T., Takami, Y., Nakayama, T., and Oshimura, M. (2004). Dicer is essential for formation of the heterochromatin structure in vertebrate cells. Nat. Cell Biol. *6*, 784–791.

Gillett, E.S., Espelin, C.W., and Sorger, P.K. (2004). Spindle checkpoint proteins and chromosome-microtubule attachment in budding yeast. J. Cell Biol. *164*, 535–546.

Gorbsky, G.J., Chen, R.H., and Murray, A.W. (1998). Microinjection of antibody to Mad2 protein into mammalian cells in mitosis induces premature anaphase. J. Cell Biol. *141*, 1193–1205.

Hagting, A., Den Elzen, N., Vodermaier, H.C., Waizenegger, I.C., Peters, J.M., and Pines, J. (2002). Human securin proteolysis is controlled by the spindle checkpoint and reveals when the APC/C switches from activation by Cdc20 to Cdh1. J. Cell Biol. *157*, 1125–1137.

Hayashi, S., and McMahon, A.P. (2002). Efficient recombination in diverse tissues by a tamoxifen-inducible form of Cre: A tool for temporally regulated gene activation/inactivation in the mouse. Dev. Biol. *244*, 305–318.

Hoyt, M.A., Totis, L., and Roberts, B.T. (1991). S. cerevisiae genes required for cell cycle arrest in response to loss of microtubule function. Cell *66*, 507–517.

Huang, H., Feng, J., Famulski, J., Rattner, J.B., Liu, S.T., Kao, G.D., Muschel, R., Chan, G.K., and Yen, T.J. (2007). Tripin/hSgo2 recruits MCAK to the inner centromere to correct defective kinetochore attachments. J. Cell Biol. *177*, 413–424.

Hussein, D., and Taylor, S.S. (2002). Farnesylation of Cenp-F is required for G2/M progression and degradation after mitosis. J. Cell Sci. *115*, 3403–3414.

Iwanaga, Y., Chi, Y.H., Miyazato, A., Sheleg, S., Haller, K., Peloponese, J.M., Jr., Li, Y., Ward, J.M., Benezra, R., and Jeang, K.T. (2007). Heterozygous deletion of mitotic arrest-deficient protein 1 (MAD1) increases the incidence of tumors in mice. Cancer Res. *67*, 160–166.

Johnson, V.L., Scott, M.I., Holt, S.V., Hussein, D., and Taylor, S.S. (2004). Bub1 is required for kinetochore localization of BubR1, Cenp-E, Cenp-F and Mad2, and chromosome congression. J. Cell Sci. *117*, 1577–1589.

Kalitsis, P., Earle, E., Fowler, K.J., and Choo, K.H. (2000). Bub3 gene disruption in mice reveals essential mitotic spindle checkpoint function during early embryogenesis. Genes Dev. *14*, 2277–2282.

Kalitsis, P., Fowler, K.J., Griffiths, B., Earle, E., Chow, C.W., Jamsen, K., and Choo, K.H. (2005). Increased chromosome instability but not

cancer predisposition in haploinsufficient Bub3 mice. Genes Chromosomes Cancer *44*, 29–36.

Kawashima, S.A., Tsukahara, T., Langegger, M., Hauf, S., Kitajima, T.S., and Watanabe, Y. (2007). Shugoshin enables tension-generating attachment of kinetochores by loading Aurora to centromeres. Genes Dev. *21*, 420–435.

Kitajima, T.S., Hauf, S., Ohsugi, M., Yamamoto, T., and Watanabe, Y. (2005). Human Bub1 defines the persistent cohesion site along the mitotic chromosome by affecting Shugoshin localization. Curr. Biol. *15*, 353–359.

Kitajima, T.S., Kawashima, S.A., and Watanabe, Y. (2004). The conserved kinetochore protein shugoshin protects centromeric cohesion during meiosis. Nature *427*, 510–517.

Kitajima, T.S., Sakuno, T., Ishiguro, K., Iemura, S., Natsume, T., Kawashima, S.A., and Watanabe, Y. (2006). Shugoshin collaborates with protein phosphatase 2A to protect cohesin. Nature *441*, 46–52.

Kops, G.J., Foltz, D.R., and Cleveland, D.W. (2004). Lethality to human cancer cells through massive chromosome loss by inhibition of the mitotic checkpoint. Proc. Natl. Acad. Sci. USA *101*, 8699–8704.

Li, R., and Murray, A.W. (1991). Feedback control of mitosis in budding yeast. Cell *66*, 519–531.

Loonstra, A., Vooijs, M., Beverloo, H.B., Allak, B.A., van Drunen, E., Kanaar, R., Berns, A., and Jonkers, J. (2001). Growth inhibition and DNA damage induced by Cre recombinase in mammalian cells. Proc. Natl. Acad. Sci. USA *98*, 9209–9214.

Meraldi, P., Draviam, V.M., and Sorger, P.K. (2004). Timing and checkpoints in the regulation of mitotic progression. Dev. Cell *7*, 45–60.

Meraldi, P., and Sorger, P.K. (2005). A dual role for Bub1 in the spindle checkpoint and chromosome congression. EMBO J. *24*, 1621–1633.

Michel, L.S., Liberal, V., Chatterjee, A., Kirchwegger, R., Pasche, B., Gerald, W., Dobles, M., Sorger, P.K., Murty, V.V., and Benezra, R. (2001). MAD2 haplo-insufficiency causes premature anaphase and chromosome instability in mammalian cells. Nature *409*, 355–359.

Morrow, C.J., Tighe, A., Johnson, V.L., Scott, M.I., Ditchfield, C., and Taylor, S.S. (2005). Bub1 and aurora B cooperate to maintain BubR1-mediated inhibition of APC/CCdc20. J. Cell Sci. *118*, 3639–3652.

Musacchio, A., and Salmon, E.D. (2007). The spindle-assembly checkpoint in space and time. Nat. Rev. Mol. Cell Biol. *8*, 379–393.

Nagy, A., Gertsenstein, M., Vintersten, K., and Behringer, R. (2003). Manipulating the Mouse Embryo: A Laboratory Manual, Third Edition (New York: Cold Spring Harbor Laboratory Press).

Peters, J.M. (2006). The anaphase promoting complex/cyclosome: A machine designed to destroy. Nat. Rev. Mol. Cell Biol. *7*, 644–656.

Putkey, F.R., Cramer, T., Morphew, M.K., Silk, A.D., Johnson, R.S., McIntosh, J.R., and Cleveland, D.W. (2002). Unstable kinetochore-microtubule capture and chromosomal instability following deletion of CENP-E. Dev. Cell *3*, 351–365.

Riedel, C.G., Katis, V.L., Katou, Y., Mori, S., Itoh, T., Helmhart, W., Galova, M., Petronczki, M., Gregan, J., Cetin, B., et al. (2006). Protein phosphatase 2A protects centromeric sister chromatid cohesion during meiosis I. Nature *441*, 53–61.

Salic, A., Waters, J.C., and Mitchison, T.J. (2004). Vertebrate shugoshin links sister centromere cohesion and kinetochore microtubule stability in mitosis. Cell *118*, 567–578.

Silver, D.P., and Livingston, D.M. (2001). Self-excising retroviral vectors encoding the Cre recombinase overcome Cre-mediated cellular toxicity. Mol. Cell *8*, 233–243.

Tang, Z., Shu, H., Qi, W., Mahmood, N.A., Mumby, M.C., and Yu, H. (2006). PP2A is required for centromeric localization of Sgo1 and proper chromosome segregation. Dev. Cell *10*, 575–585.

Tang, Z., Sun, Y., Harley, S.E., Zou, H., and Yu, H. (2004). Human Bub1 protects centromeric sister-chromatid cohesion through Shugoshin during mitosis. Proc. Natl. Acad. Sci. USA *101*, 18012–18017.

Taylor, S.S., Ha, E., and McKeon, F. (1998). The human homologue of Bub3 is required for kinetochore localization of Bub1 and a Mad3/Bub1-related protein kinase. J. Cell Biol. *142*, 1–11.

Taylor, S.S., Hussein, D., Wang, Y., Elderkin, S., and Morrow, C.J. (2001). Kinetochore localisation and phosphorylation of the mitotic checkpoint components Bub1 and BubR1 are differentially regulated by spindle events in human cells. J. Cell Sci. *114*, 4385–4395.

Taylor, S.S., and McKeon, F. (1997). Kinetochore localization of murine Bub1 is required for normal mitotic timing and checkpoint response to spindle damage. Cell *89*, 727–735.

Vanoosthuyse, V., Prykhozhij, S., and Hardwick, K.G. (2007). Shugoshin 2 regulates localization of the chromosomal passenger proteins in fission yeast mitosis. Mol. Biol. Cell *18*, 1657–1669.

Wang, Q., Liu, T., Fang, Y., Xie, S., Huang, X., Mahmood, R., Ramaswamy, G., Sakamoto, K.M., Darzynkiewicz, Z., Xu, M., and Dai, W. (2004). BUBR1 deficiency results in abnormal megakaryopoiesis. Blood *103*, 1278–1285.

Warren, C.D., Brady, D.M., Johnston, R.C., Hanna, J.S., Hardwick, K.G., and Spencer, F.A. (2002). Distinct chromosome segregation roles for spindle checkpoint proteins. Mol. Biol. Cell *13*, 3029–3041.

Weaver, B.A., Bonday, Z.Q., Putkey, F.R., Kops, G.J., Silk, A.D., and Cleveland, D.W. (2003). Centromere-associated protein-E is essential for the mammalian mitotic checkpoint to prevent aneuploidy due to single chromosome loss. J. Cell Biol. *162*, 551–563.